Sites and Mechanisms of Aconitase Inactivation by Peroxynitrite: Modulation by Citrate and Glutathione†

Derick Han,‡ Raffaella Canali,§ Jerome Garcia,|| Rodrigo Aguilera,|| Timothy K. Gallaher,|| and Enrique Cadenas*,||

Research Center for Liver Disease, Keck School of Medicine, University of Southern California, 2011 Zonal Avenue, Los Angeles, California 90089-9121, Istituto Nazionale Ricerca Alimenti e Nutrizione, via Ardeatina 546, 00178 Rome, Italy, and Department of Molecular Pharmacology and Toxicology, School of Pharmacy, University of Southern California, 1985 Zonal Avenue, Los Angeles, California 90089-9121

Received May 20, 2005; Revised Manuscript Received July 15, 2005

ABSTRACT: Aconitases are iron−sulfur cluster-containing proteins present both in mitochondria and cytosol of cells; the cubane iron−sulfur (Fe−S) cluster in the active site is essential for catalytic activity, but it also renders aconitase highly vulnerable to reactive oxygen and nitrogen species. This study examined the sites and mechanisms of aconitase inactivation by peroxynitrite ($ONOO^-$), a strong oxidant and nitrating agent readily formed from superoxide anion and nitric oxide generated by mitochondria. $ONOO^-$ inactivated aconitase in a dose-dependent manner (half-maximal inhibition was observed with ~3 μM $ONOO^-$). Low levels of $ONOO^-$ caused the conversion of the Fe−S cluster from the $[4Fe-4S]^{2+}$ form to the inactive $[3Fe-4S]^{1+}$ form with the loss of labile iron, as confirmed by low-temperature EPR analysis. In the presence of the substrate, citrate, 66-fold higher concentrations of $ONOO^-$ were required for half-maximal inhibition. The protective effects of citrate corresponded to its binding to the active site. The inactivation of aconitase in the presence of citrate was due to $ONOO^-$-mediated cysteine thiol loss and tyrosine nitration in the enzyme as shown by Western blot analyses. LC/MS/MS analyses revealed that $ONOO^-$ treatment to aconitase resulted in nitration of tyrosines 151 and 472 and oxidation to sulfonic acid of cysteines 126 and 385. The latter is one of the three cysteine residues in aconitase that binds to the Fe−S cluster. All other modified tyrosine and cysteine residues were adjacent to the binding site, thus suggesting that these modifications caused conformational changes leading to active-site disruption. Aconitase cysteine thiol modifications other than oxidation to sulfonic acid, such as S-glutathionylation, also decreased aconitase activity, thus indicating that glutathionylation may be an important means of modulating aconitase activity under oxidative and nitrative stress. Taken together, these results demonstrate that the Fe−S cluster in the active site, cysteine 385 bound to the Fe−S cluster, and tyrosine and cysteine residues in the vicinity of the active site are important targets of oxidative and/or nitrative attack, which is selectively controlled by the mitochondrial matrix citrate levels. The mechanisms inherent in aconitase inactivation by $ONOO^-$ are discussed in terms of the mitochondrial matrix metabolic and thiol redox state.

Aconitases [citrate (isocitrate) hydrolyase, EC 4.2.1.4] are iron−sulfur cluster-containing proteins present both in mitochondria and cytosol of cells; the enzymes catalyze the stereospecific conversion of citrate to isocitrate via the intermediate formation of *cis*-aconitate (*1*, *2*). The cubane $[4Fe-4S]^{2+}$ cluster in the active site is essential for catalytic activity, but it also renders aconitase highly vulnerable to reactive oxygen and nitrogen species (*3*, *4*). Three of the iron atoms in the cubane structure are bound to cysteine sulfurs of the protein backbone; the fourth iron (Fe_α) is ligated to inorganic sulfur and participates in the binding of the substrate to the active site (*1*, *2*, *5*). Superoxide anion ($O_2^{\cdot-}$), hydrogen peroxide (H_2O_2), and peroxynitrite ($ONOO^-$) have been shown to inactivate mitochondrial aconitase through modifications of the $[4Fe-4S]^{2+}$ cluster (*4*−*7*). $ONOO^-$ is believed to disrupt the Fe−S cluster by causing a loss of labile Fe from the cluster resulting in an inactive $[3Fe-4S]^{1+}$ form (*4*). However, direct measurements confirming the nature of $ONOO^-$-mediated modifications of the Fe−S cluster have not been obtained yet.

$ONOO^-$ may also modulate aconitase activity through modifications of amino acids, such as cysteine and tyrosine. Aconitase contains 12 cysteine residues, with three contributing ligands to the [Fe−S] cluster and one cysteine residing in the active site (*1*, *8*). Although the latter is not essential for aconitase activity, its binding to various agents [e.g., NEM, *N*-ethylmaleimide; DTNB, 5,5′-dithiobis(2-nitrobenzoic acid)] results in a decrease aconitase activity, probably by inhibiting citrate entry to the active site (*1*, *8*). Because

† This work was supported by Grants RO1 ES011342 and RO1 AG16718 from NIH. R.C. was partially supported by a grant from Horphag Res., Ltd.

* To whom correspondence should be addressed: Molecular Pharmacology and Toxicology, School of Pharmacy, University of Southern California, Los Angeles, CA 90089-9121. Telephone: +1-323-442-1418. Fax +1-323-224-7473. E-mail cadenas@usc.edu.

‡ Keck School of Medicine, University of Southern California.

§ Istituto Nazionale Ricerca Alimenti e Nutrizione.

|| School of Pharmacy, University of Southern California.

10.1021/bi0509393 CCC: $30.25
Published on Web 08/18/2005

thiol residues can be oxidized by $ONOO^-$ and H_2O_2 (*5*, *9*), they remain potential targets of oxidative attack. The reaction of $ONOO^-$ with thiols generates primarily a thiyl radical (reaction 1), which may decay to a sulfenic acid (reaction 3) via a nitrated sulfur intermediate (reaction 2) (*10*).

$$RSH + [HO^{\cdot}\cdots NO_2^{\cdot}] \rightarrow RS^{\cdot} + NO_2^{\cdot} + H_2O \quad (1)$$

$$RS^{\cdot} + NO_2^{\cdot} \rightarrow RSNO_2 \quad (2)$$

$$RSNO_2 + OH^- \rightarrow RSOH + NO_2^- \quad (3)$$

Tyrosine residues react with $ONOO^-$ to form 3-nitrotyrosine as the major product (reactions 4 and 5 show one possible mechanism) (*11*). Aconitase contains 22 tyrosine residues, and whether nitrotyrosine formation in some of these residues may affect enzyme activity remains to be determined.

$$R\text{-}TyrH + [HO^{\cdot}\cdots NO_2^{\cdot}] \rightarrow RTyr^{\cdot} + NO_2^{\cdot} + H_2O \quad (4)$$

$$RTyr^{\cdot} + NO_2^{\cdot} \rightarrow R\text{-}Tyr\text{-}NO_2 \quad (5)$$

Appreciation of the mechanisms inherent in aconitase inactivation by $ONOO^-$ in a cellular setting requires consideration of enzyme substrate availability and the pathways of $ONOO^-$ formation in mitochondria. Cysteine and tyrosine residues of aconitase may be important targets of oxidant attack, because the [Fe−S]-containing active site of aconitase may be protected by citrate in a cellular setting. It has been shown that the presence of citrate can protect the thiol residues in the active site from thiol alkylating agents, such as NEM (*8*), and shield the Fe−S cluster from inactivation by $O_2^{\cdot-}$ (*12*). Whether citrate may sterically block the Fe−S cluster from $ONOO^-$ in a similar fashion, thereby rendering amino acid residues vulnerable to oxidation, has not been explored.

Mitochondria are important sources of $ONOO^-$, because the mitochondrial respiratory chain (*13*, *14*) and the inner membrane-associated mitochondrial nitric oxide synthase (*15*−*17*) furnish both reactants, $O_2^{\cdot-}$ and $^{\cdot}NO$, required for $ONOO^-$ formation ($O_2^{\cdot-} + {}^{\cdot}NO \rightarrow ONOO^-$), a reaction that proceeds at diffusion-controlled rates. In addition, $^{\cdot}NO$ regulates both mitochondrial respiration and $O_2^{\cdot-}$ production by its reversible binding to cytochrome oxidase (*18*−*20*) and inhibition of electron transfer at the bc_1 segment (*21*, *22*), respectively. $ONOO^-$, thus formed, has been reported to inhibit complex I activity (*23*, *24*), stimulate inner membrane proton permeability (*25*), trigger cytochrome *c* release to regulate apoptosis (*26*), and appears to contribute to the pathology of many diseases including Alzheimer's disease, myocardial ischemia, and amyotrophic lateral sclerosis (*27*). Similarly, $O_2^{\cdot-}$ diffusing from mitochondria to cytosol via voltage-dependent anion channels (*28*) can combine with $^{\cdot}NO$ to yield $ONOO^-$ in cytosol, thus widening the spectrum of protein targets (among them cytosolic aconitase) of this powerful oxidant.

In this study, the sites and mechanisms of aconitase inactivation by $ONOO^-$ were examined using a porcine aconitase preparation: the role of citrate in $ONOO^-$-mediated damage of aconitase iron−sulfur cluster and amino acids was investigated, and specific targets for $ONOO^-$-mediated oxidation and nitration were identified. The significance of these mechanisms within the context of the mitochondrial thiol/disulfide status was assessed in terms of the sensitivity of aconitase to glutathionylation.

EXPERIMENTAL PROCEDURES

Chemicals. 4-(2-Hydroxyethyl)piperazine-1-ethanesulfonic acid (HEPES), ethylenediaminetetraacetic acid (EDTA), bovine serum albumin, dithiothreitol (DTT),[1] ascorbic acid, $NADP^+$, 5,5-dimethyl-1-pyrolline-*N*-oxide (DMPO), 3-morpholino-sydnonimine (SIN-1), and DTNB [5,5′-dithiobis(2-nitrobenzoic acid)] were from Sigma Chemical Co. (St Louis, MO). Supelco P-10 sephadex G-25 columns were from Amersham Pharmacia Biotech (Piscataway, NJ). Peroxynitrite ($ONOO^-$) was obtained from Upstate (Waltham, MA). All other reagents were of analytical grade. A water solution of DMPO containing 0.1 mM DETAPAC (diethyenetriamine-pentaacetic acid) was purified several times with activated charcoal; the DMPO concentration was calculated spectrophotometrically ($\epsilon_{232} = 7700\ M^{-1}\ cm^{-1}$); and the stock solution was kept under He at −20 °C. The $ONOO^-$ concentration was verified on the day of the experiment by UV absorption spectrometry ($\epsilon_{302} = 1670\ M^{-1}\ cm^{-1}$).

Porcine aconitase preparations obtained from Sigma Chemical Co. (St Louis, MO) had been similarly used in a previous study involving $ONOO^-$ (*4*). Analysis of the aconitase preparation using SDS gel and mass spectometry revealed the fraction to contain other proteins, particularly porcine serum albumin used to stabilize aconitase. Therefore, mass spectrometry was used to confirm the identity and purity of the aconitase band used in Western blot analysis.

Aconitase Assay. Porcine heart aconitase (15 mg) was activated in a reaction containing 0.5 mM ferrous ammonium sulfate and 5 mM DTT buffered with 100 mM Tris-HCl at pH 7.5 and incubated under He at 0 °C for 30 min. Activated aconitase was rapidly separated on Sephadex G-25 preequilibrated with He-saturated 100 mM Tris/HCl at pH 7.5 (*29*). Aliquots of activated aconitase were stored under He at −80 °C. Aconitase activity was assayed on a reaction mixture consisting of 50 mM Tris-HCl at pH 7.4, 30 mM sodium citrate, 0.6 mM $MnCl_2$, 0.2 mM $NADP^+$, and 1 unit/mL of isocitrate dehydrogenase; the reaction was followed at 340 nm ($\epsilon_{340} = 6.22\ mM^{-1}\ cm^{-1}$) for 10 min at room temperature. An aconitase activity of 1 mU corresponded to 1 nmol NADPH formed per minute (*30*).

Aconitase (2 mU/mL) in 50 mM Tris-HCl at pH 7.4 was treated with varying amounts of $ONOO^-$. During the addition of $ONOO^-$, the aconitase-containing solution was rapidly vortexed to ensure complete mixing before significant decomposition of $ONOO^-$ occurred. Aconitase activity was measured immediately after mixing.

For experiments involving SIN-1, aconitase samples were incubated at room temperature with varying amounts of SIN-1 for 10 min. To remove SIN-1 from aconitase, treated samples were spun in a micro bio-spin desalting column (Biorad, Hercules, CA) for 4 min at 4 °C. The desalted samples were immediately analyzed for aconitase activity. Aconitase samples treated with glutathione disulfide (GSSG)

[1] Abbreviations: GSSG, glutathione disulfide, DTT, dithiotreitol; DMPO, 5,5-dimethyl-1-pyrroline-*N*-oxide; maleimide PEO_2−biotin, (+)-biotinyl-3-maleimidopropionamidyl-3,6-dioxa-octanediamine.

were preincubated for 10 min with GSSG before aconitase activity was assessed. Control experiments were performed to verify that GSSG did not affect isocitrate dehydrogenase activity. In samples treated with DTT, aconitase was incubated with citrate and GSSG followed by a 10-min treatment with 10 mM DTT. The presence of citrate was required when working with DTT, because DTT directly affected the active site of aconitase.

Immunoblotting for Protein Thiols, Glutathionylation, and Nitrotyrosine. Aconitase preparations (4 mU/mL) were treated with either $ONOO^-$ or GSSG in 50 mM Tris-HCl at pH 7.4 and run on an 8% SDS−PAGE nonreducing gel. Western blot analysis for nitrotyrosine in aconitase was determined with an anti-nitrotyrosine antibody (Upstate, Charlottesville, VA). Glutathionylation of aconitase was assessed by Western blotting using an anti-glutathione monoclonal antibody (Virogen, Watertown, MA) (*31*) after incubation with various concentrations of GSSG for 10 min. Changes in aconitase protein thiols were determined by labeling the enzyme with (+)-biotinyl-3-maleimidopropionamidyl-3,6-dioxa-octanediamine (maleimide PEO_2-biotin, 20 mM; Pierce, Rockford, IL) for 1 h. Western blot analysis of biotinylated proteins was subsequently performed using a streptavidin antibody (Pierce, Rockford, IL). Band densities were estimated with a Versadoc Image System (BioRad, Hercules, CA). The band corresponding to aconitase in all Western blots was confirmed by LC/MS/MS analysis.

LC/MS/MS: (a) In-Gel Tryptic Digest. Protein spots from SDS−PAGE were excised from the gels using biopsy punches (Acuderm). In-gel tryptic digest was carried out using trypsin that was reductively methylated to reduce autolysis (Promega, Madison, WI). Prior to digestion, samples were neither reduced with DTT nor alkylated with iodoacetamide to keep potential cysteine modifications stable. The digestion reaction was carried out overnight at 37 °C. Digestion products were extracted from the gel with a 5% formic acid/50% acetonitrile solution (2×) and one acetonitrile extraction followed by evaporation using an APD SpeedVac (ThermoSavant).

(b) Analysis of Tryptic Peptide Sequence Tags by Tandem Mass Spectrometry. The dried tryptic digest samples were cleaned with ZipTip and resuspended in 10 μL of 60% formic acid. Chromatographic separation of the tryptic peptides was achieved using a ThermoFinnigan Surveyor MS-Pump in conjunction with a BioBasic-18 100 × 0.18 mm reverse-phase capillary column (ThermoFinnigan, San Jose, CA). Mass analysis was done using a ThermoFinnigan LCQ Deca XP Plus ion trap mass spectrometer equipped with a nanospray ion source (ThermoFinnigan) employing a 4.5-cm long metal needle (Hamilton, 950-00954) using a data-dependent acquisition mode. Electrical contact and voltage application to the probe tip took place via the nanoprobe assembly. Spray voltage of the mass spectrometer was set to 2.9 kV and heated capillary temperature at 190 °C. The column equilibrated for 5 min at 1.5 μL/min with 95% solution A and 5% solution B (A, 0.1% formic acid in water; B, 0.1% formic acid in acetonitrile) prior to sample injection. A linear gradient was initiated 5 min after sample injection ramping to 35% A and 65% B after 50 min and 20% A and 80% B after 60 min. Mass spectra were acquired in the *m*/*z* 400−1800 range.

(*c*) *Protein Identification*. Protein identification was carried out with the MS/MS search software Mascot 1.9 (Matrix Science) with confirmatory or complementary analyses with TurboSequest as implemented in the Bioworks Browser 3.2, build 41 (ThermoFinnigan). NCBI Sus scrofa protein sequences were used as the primary search database, and searches were complemented with the NCBI nonredundant protein database. Each MS/MS spectrum was analyzed for methionine and cysteine oxidation (+16), tryptophan and tyrosine nitration (+45), and cysteine and tryptophan for dioxidation and trioxidation (+32 and +48) as specific differential modifications. Aconitase amino acid numbering is based on the Sus scrofa reference sequence NP 999119; for comparison with the amino acid numbering in the reported crystal structure of aconitase (*32*), it should be considered that the first amino acid in the crystal structure is number 28 in the reference sequence at NCBI. The aconitase structure shown in Figure 7 was generated with the WebLab Viewer Pro 3.7 (Molecular Simulations, Inc., San Diego, CA) from the Protein Data Bank (Structure explorer, 6ACN) based on the aconitase crystal structure (*32*).

Electron Paramagnetic Resonance (EPR): (a) DMPO/Cysteinyl Radical−Protein Spin Adduct measurements. EPR spectra were recorded with a Brucker ECS 106 spectrometer, equipped with a TM^{110} room-temperature cavity. Spectra acquisition began 2 min after the rapid mixing of $ONOO^-$ (0.75 mM) into a mixture containing 50 mU/mL aconitase and 65 mM DMPO in 100 mM Tris-HCl at pH 7.5. Instrument settings: microwave frequency, 9.77 GHz; microwave power, 20 mW; field modulation frequency, 100 kHz; field modulation amplitude, 2 G; receiver gain, 8×10^5; time constant, 328 ms; scan rate, 0.9 G s^{-1}; and number of scans accumulated, 5. Experiments were performed at room temperature. Computer simulations of spectra were performed using the WinSIM program (EPR calculations for MS-Windows NT 95, version 0.96, from P.E.S.T., Public EPR Software Tools) (*33*).

(b) Glutathionyl Radical ($GS^{\cdot}$) Measurements. Spectra were recorded 1 min after the rapid mixing of $ONOO^-$ (0.7 mM) in 100 mM Tris HCl at pH 7.5 containing 18 mM GSH, 52 mM DMPO, and different concentrations of aconitase. The EPR signal intensities were calculated by double integration of the 3470 G line. Instrument settings: microwave frequency, 9.77 GHz; microwave power, 20 mW; field modulation frequency, 100 kHz; field modulation amplitude, 1 G; receiver gain, 8×10^5; time constant, 82 ms; and scan rate, 1.9 G s^{-1}. Experiments were performed at room temperature.

(c) Aconitase $[3Fe-4S]^{1+}$ Measurements. The active form of aconitase ($[4Fe-4S]^{2+}$) is EPR silent, whereas the inactive aconitase form ($[3Fe-4S]^{1+}$) shows an EPR signature at $g \sim 2.02$ at low temperatures (*34*). EPR spectra were recorded at 10 K. Aconitase suspensions (50 mU/mL) were rapidly mixed with various concentrations of $ONOO^-$ in 100 mM Tris-HCl at pH 7.5 and frozen in liquid nitrogen before measurements. Instrument settings: microwave frequency, 9.177 GHz; microwave power, 100 mW; field modulation frequency, 100 kHz; modulation amplitude, 0.5 mT; and number of scans accumulated, 5.

RESULTS

Aconitase Inactivation by ONOO⁻: Protective Effect of Citrate. Treatment of the porcine heart aconitase preparation with $ONOO^-$ resulted in a dose-dependent loss of aconitase activity (Figure 1A). In the absence of citrate, the enzyme substrate, half-maximal inhibition was observed with ~3 μM $ONOO^-$. Citrate significantly protected aconitase against inactivation by $ONOO^-$, with ~66-fold higher levels of the oxidant (200 μM) being required to elicit a 50% inhibition of enzyme activity. The treatment of aconitase with SIN-1, which generates a continuous flow of $ONOO^-$, similarly inactivated aconitase, with citrate having a protective effect (Figure 1B). The difference in dose−response curves observed for $ONOO^-$ and SIN-1 may be explained as a lack of linear dependence between $ONOO^-$ produced and the SIN-1 concentration (*35*). All subsequent experiments were performed with known concentrations of $ONOO^-$.

The difference in the $ONOO^-$ concentration needed to inactivate aconitase in the absence and presence of citrate suggests that two different sites on aconitase can be affected by $ONOO^-$: (a) the Fe−S cluster in the active site, which is sensitive to low levels of $ONOO^-$ (*4*) and is protected by citrate, and (b) amino acid residues, which are less sensitive to $ONOO^-$ and cannot be protected by citrate. To determine if the doses of citrate required to protect aconitase from $ONOO^-$ were associated with the binding of citrate to the active site, a dose−response curve was performed (Figure 1C). The K_M of citrate for aconitase was estimated as 33 μM (*3*). The percent of the aconitase active site occupied with citrate ($\%_{aconitase-citrate}$) is given by the equation

$$\%_{aconitase-citrate} = [citrate]/[citrate] + K_M$$

The protective effects of citrate tallied its binding to the active site of aconitase (Figure 1C). These results confirm that citrate protects aconitase by sterically blocking $ONOO^-$ access to the Fe−S cluster-containing active site.

Modification of the Fe−S Cluster by ONOO⁻. The modification of the Fe−S cluster in the active site of aconitase by low doses of $ONOO^-$ was confirmed by EPR spectroscopy. The active $[4Fe-4S]^{2+}$ cluster of aconitase is EPR silent, but when converted to the inactive $[3Fe-4S]^{1+}$ form, it becomes detectable by EPR at low temperatures (*34*). Untreated aconitase contained a small EPR signal (Figure 2A). Both low (30 μM) (Figure 2B) and high (500 μM) (Figure 2C) levels of $ONOO^-$ yielded an EPR signal characteristic of aconitase in the $[3Fe-4S]^{1+}$ form. Higher $ONOO^-$ concentrations (>1 mM) caused a loss of the EPR signal (Figure 2D), thus indicating the further degradation of the $[3Fe-4S]^{1+}$ cluster to an EPR-silent form. Because high concentrations of aconitase (50 mU/mL) are necessary for EPR analysis, corresponding high levels of citrate and $ONOO^-$ were used. Citrate protected aconitase from $ONOO^-$ inactivation (Figure 2E). These results support the notion that low levels of $ONOO^-$ inactivated the enzyme upon modification of the [Fe−S] cluster at the active site ($[4Fe-4S]^{2+} \rightarrow [3Fe-4S]^{1+}$) and that citrate protected the Fe−S cluster from damage. In the presence of citrate, however, the inactivation of aconitase by $ONOO^-$ (parts A and B of Figure 1) is likely due to its reaction at a site other than the Fe−S cluster-containing active site.

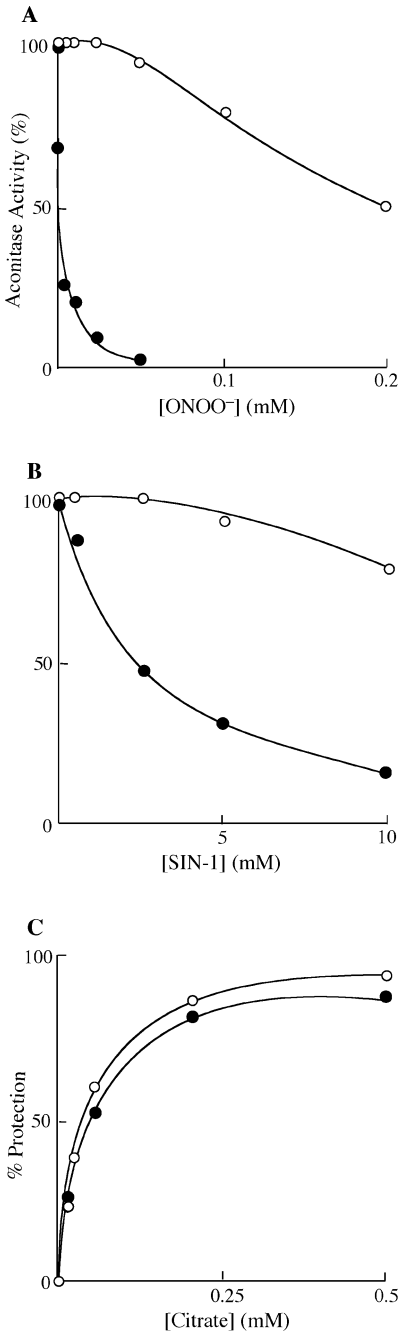

FIGURE 1: $ONOO^-$-mediated inactivation of aconitase. Effect of citrate. (A) $ONOO^-$-mediated inactivation of aconitase. Porcine aconitase (2 mU/mL) in 50 mM Tris-HCl at pH 7.4 was rapidly mixed with varying amounts of $ONOO^-$ in the absence (●) or presence (○) of 2.5 mM citrate. (B) SIN-1-mediated inactivation of aconitase. Porcine aconitase (2 mU/mL) in 50 mM Tris-HCl at pH 7.4 was incubated with varying concentrations of SIN-1 for 10 min in the absence (●) or presence (○) of 2.5 mM citrate. To remove SIN-1, samples were spun down in a micro bio-spin desalting column for 4 min at 4 °C and immediately analyzed for aconitase activity. (C) Dose−response curve of citrate protection against $ONOO^-$-mediated inactivation of aconitase. Porcine aconitase (2 mU/mL) was rapidly mixed with varying amounts of citrate and $ONOO^-$ (200 μM). (○) Measured percent protection by citrate against $ONOO^-$. (●) Estimated percentage of aconitase active site occupied by citrate. The percent of citrate binding to aconitase was calculated using the equation in the text. The K_M of aconitase for citrate was estimated as 33 μM.

Spin Trapping of an Immobilized Protein Thiyl Radical. To assess if $ONOO^-$ inactivation of aconitase in the presence

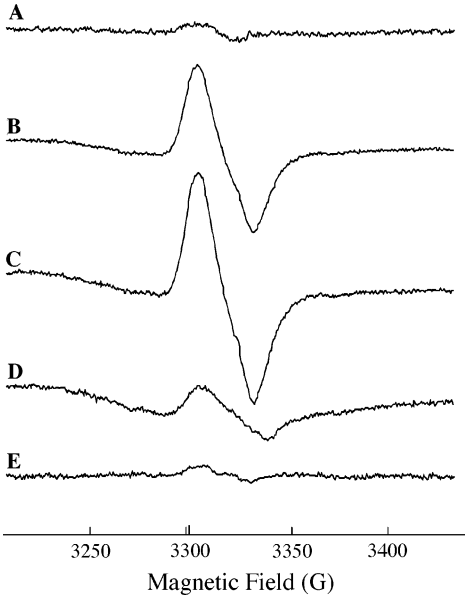

FIGURE 2: Effect $ONOO^-$ on the Fe−S cluster in the active site of aconitase. EPR analysis. Active aconitase contains an EPR-silent $[4Fe-4S]^{2+}$ cluster that becomes EPR-detectable when converted to the inactive $[3Fe-4S]^{1+}$ form. Aconitase (50 mU/mL) was rapidly mixed with various concentrations of $ONOO^-$ in 100 mM Tris-HCl buffer at pH 7.5 and frozen under liquid nitrogen before measurements. Measurements were performed at 10 K with instrument settings as described in the Experimental Procedures. (A) Aconitase, untreated. (B) Aconitase treated with 30 μM $ONOO^-$. (C) Aconitase treated with 500 μM $ONOO^-$. (D) Aconitase treated with 1 mM $ONOO^-$. (E) Aconitase treated with 500 μM $ONOO^-$ plus citrate (50 mM).

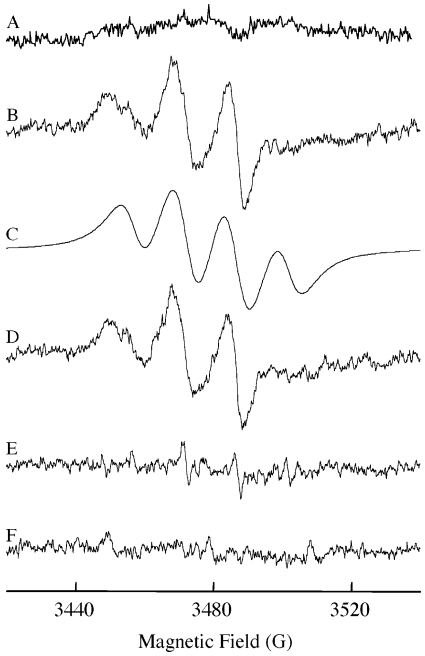

FIGURE 3: Detection of an immobilized DMPO/cysteinyl radical−protein radical adduct after $ONOO^-$ treatment. Aconitase (50 mU/mL) was rapidly mixed with various concentrations of $ONOO^-$ in 50 mM Tris/HCl at pH 7.5 containing 65 mM DMPO. (A) Aconitase treated with 25 μM $ONOO^-$. (B) Aconitase treated with 500 μM $ONOO^-$. (C) Computer simulation of B ($r = 0.802$) assuming $a_N = 14.5$ G, $a^{\beta}_H = 15.6$ G, and line width = 7.7 G. (D) Aconitase treated with 500 μM $ONOO^-$ plus 200 mM citrate. (E) $ONOO^-$ (500 μM) in the absence of aconitase. (F) Aconitase pretreated with 2 mM NEM (2 mM) *prior* to treatment of 500 μM $ONOO^-$.

of citrate was due to modification of cysteine residues, EPR in conjunction with the spin-trap DMPO was used. The interaction of thiols (RSH) with $ONOO^-$ (or its protonated form, which disassociates within a cage) yields mainly thiyl radicals ($RS^{\cdot}$) (reaction 1). EPR analysis with DMPO was employed to determine the formation of protein thiyl radicals during $ONOO^-$ treatment. The addition of a low concentration of $ONOO^-$ (25 μM) did not generate an EPR signal (Figure 3A), whereas the addition of a high concentration of $ONOO^-$ (500 μM) resulted in formation of a DMPO/cysteinyl radical spin adduct (Figure 3B) consisting of a broad, anisotropic EPR signal: the broad lines in the spectrum are characteristic of a slow tumbling, protein-derived radical. Figure 3C shows a computer-simulated spectrum of the DMPO/protein cysteinyl radical spin adduct ($a_N = 14.5$ G; $a^{\beta}_H = 15.6$ G; line width = 7.7 G), which matches that of the DMPO/protein cysteinyl radical adduct of hemoglobin and myoglobin previously reported (*36*, *37*). Because the aconitase preparation contained some other proteins, particularly albumin to stabilize aconitase, the DMPO/cysteinyl radical spin adduct could not be solely attributed to aconitase. However, Western blot analysis with maleimide PEO_2−biotin demonstrated that aconitase was one of the few thiol-containing proteins (data not shown), thus implying that aconitase contributed significantly to the formation of the DMPO/protein thiyl radical spin adduct. The formation of such an adduct is consistent with a mechanism entailing oxidation of −SH moieties by $ONOO^-$ to yield a thiyl radical (reaction 1). The EPR signal was not affected by high concentrations of citrate (200 μM; Figure 3D). In the absence of aconitase, $ONOO^-$ yielded a low-intensity signal probably corresponding to the spin adduct of the hydroxyl radical (Figure 3E). The protein cysteinyl radical adduct signal was abolished upon alkylation of protein thiols by NEM (Figure 3F). Because NEM binds to all thiol residues, the loss of the EPR signal upon NEM treatment confirms that the EPR spectrum originated form a thiol residue in the protein.

Reaction of $ONOO^-$ with Cysteine and Tyrosine Residues in Aconitase. Thiyl radicals generated from $ONOO^-$ (reaction 1) or other oxidants can decay to stable oxidation products, such as disulfides and sulfenic acids (reaction 3); the latter have reactive properties different from thiols. Protein thiols can be labeled using maleimide (such as maleimide PEO_2−biotin, i.e., biotinylation), while oxidized cysteine products do not bind to maleimides (i.e., cannot be biotinylated). To assess protein thiols levels after $ONOO^-$ treatment, Western blot analysis was performed using maleimide PEO_2−biotin. Figure 4A shows that thiols in aconitase are lost in a dose-dependent manner upon $ONOO^-$ treatment. Aconitase preparations that had not been labeled with maleimide PEO_2−biotin failed to show a band; this demonstrated that no endogenous biotin group(s) existed within aconitase. The presence of citrate did not prevent the loss of thiols upon $ONOO^-$ treatment (data not shown), thus strengthening the notion that cysteine oxidation occurred at sites other than the active site.

Besides cysteine, tyrosine residues represent a major target for $ONOO^-$-induced modification (reactions 4 and 5). Western blot analysis using anti-nitrotyrosine antibodies showed a dose-dependent increase in nitrotyrosine formation

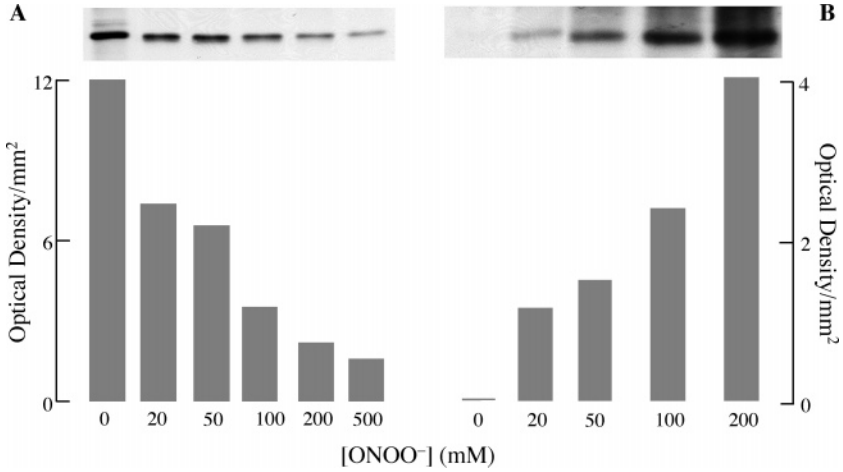

FIGURE 4: Loss of aconitase thiols and nitrotyrosine formation following $ONOO^-$ treatment. (A) Loss of aconitase protein thiols following $ONOO^-$ treatment. Porcine aconitase (4 mU/mL) was rapidly mixed with varying amounts of $ONOO^-$ in 50 mM Tris-HCl buffer at pH 7.4. The aconitase preparation was then treated with maleimide PEO_2−biotin as described in the Experimental Procedures. Samples were run on an 8% SDS−PAGE nonreducing gel, and LC/MS−MS was used to confirm the aconitase band. (Upper panel) Western blot analysis of biotinylated proteins (performed using a streptavidin antibody). (Lower panel) Semiquantitative analysis (densitometry) of Western blots. (B) Nitrotyrosine formation following $ONOO^-$ treatment. Porcine aconitase (4 mU/mL) was rapidly mixed with varying amounts of $ONOO^-$ in 50 mM Tris-HCl buffer at pH 7.4; samples were run on a SDS−PAGE (8%) nonreducing gel. LC/MS−MS was used to confirm the aconitase band. (Upper panel) Western blot analysis for nitrotyrosine (performed using a polyclonal anti-nitrotyrosine antibody). (Lower panel) Semiquantitative analysis (densitometry) of Western blots.

in aconitase with increasing $ONOO^-$ levels (Figure 4B), thus suggesting that some of the 22 tyrosyl residues in aconitase were nitrated upon treatment with $ONOO^-$. As with the protein thiols mentioned above, citrate did not prevent protein tyrosine nitration (data not shown), thus suggesting that the latter occurs even when the active site of the enzyme is occupied by its substrate and that citrate does not react with $ONOO^-$.

LC/MS/MS Analysis of Aconitase Modified by $ONOO^-$ Treatment. LC/MS/MS analysis of aconitase following $ONOO^-$ treatment revealed four amino acid modifications: oxidation of cysteines 126 and 385 to sulfonic or cysteic acid and nitration of tyrosines 151 and 472. These results confirm the Western blot analysis that revealed the loss of cysteine residues (Figure 4A) and nitrotyrosine formation (Figure 4B) as major consequences of $ONOO^-$ treatment. Cysteine 385 is one of three cysteine residues that bind the Fe−S cluster in the active site of aconitase. This suggests that aconitase may be partly inactivated by disrupting the binding of the Fe−S cluster to cysteine 385.

Sequence coverage for aconitase in both control and $ONOO^-$-treated samples was approximately 40% in samples subjected to LC/MS/MS analysis. The four amino acid modifications were observed over the course of analysis of at least six separate distinct sample preparations. In each of the four cases, tryptic peptides containing the identified modification were observed by both Mascot and Sequest analysis in at least two or more separate sample preparations and LC/MS/MS analyses. In no instance were these oxidative and nitrative modifications observed in control samples (not treated with $ONOO^-$). Table 1 summarizes the amino acid residues modified to cysteic acid or nitrotyrosine over the course of multiple sample analyses by Mascot and Sequest search software.

Tyrosine 151. Nitration of tyrosine 151 was observed in the same doubly charged 16 amino acid tryptic peptide 5 times in four separate LC/MS/MS analyses. Sequest cross correlation (XC) values ranged from 2.4 to 4.9 and Δcn values from 0.39 to 0.65 (Table 1). Retention time for the nitrotyrosine-modified peptide was consistent among separate LC/MS/MS runs, and nonmodified peptide sequences were also observed with equal or higher XC values compared to modified peptide (data not shown). A representative MS/MS spectra (XC = 4.8) is presented in Figure 5B. The precursor ion was doubly charged with a mass of 900.1 Da corresponding to a 16-residue tryptic peptide, comprising amino acids 145−160, with one nitration modification. Fragment b and y ions were observed for nearly all-observable single-charged fragments, and four of each of doubly charged b and y ions were assigned as well.

Table 1: LC/MS/MS Analysis of Aconitase Amino Acid Modifications[a]

tryptic peptide	residue	charge	MSc	XC	Δcn
		3[b]	33	2.7	0.45
VAVPSTIH**C**DHLIEAQLGGEK	Cys^{126}	3	30	2.3	0.50
		3	25	2.1	0.34
		2[b]	83	4.9	0.54
		2	81	4.8	0.56
DINQEV**Y**NFLATAGAK	Tyr^{151}	2	73	4.0	0.65
		2	59	4.3	0.65
		2	13	2.4	0.39
		2[b]	64	4.6	0.71
VGLIGS**C**TNSSYED**M**GR	Cys^{385}	2	57	4.0	0.59
		2	54	4.3	0.64
		2	43	4.3	0.66
		2[b]	33	2.5	0.54
NTIVTS**Y**NR	Tyr^{472}	2	33	2.4	0.62
		2	27	2.0	0.24

[a] Aconitase amino acids modified upon treatment with $ONOO^-$. Experiments were carried out with 4 mU/mL aconitase supplemented with 300 μM $ONOO^-$. Included are the tryptic peptide fragment sequence, peptide charge, Mascot Ions Score (MSc), Sequest XC, and Δcn value. Δcn is the difference in the cross correlation score between the top two candidate peptides or proteins for a given input data file. Charge and score values are presented for each instance of identification over the course of at least six proteomic analyses. Residues were determined from the spectra in Figure 5. [b] Spectra shown in Figure 5.

Cysteine 385. Cysteine 385, one of the three cysteine residues to bind the Fe−S cluster, was oxidized to cysteic

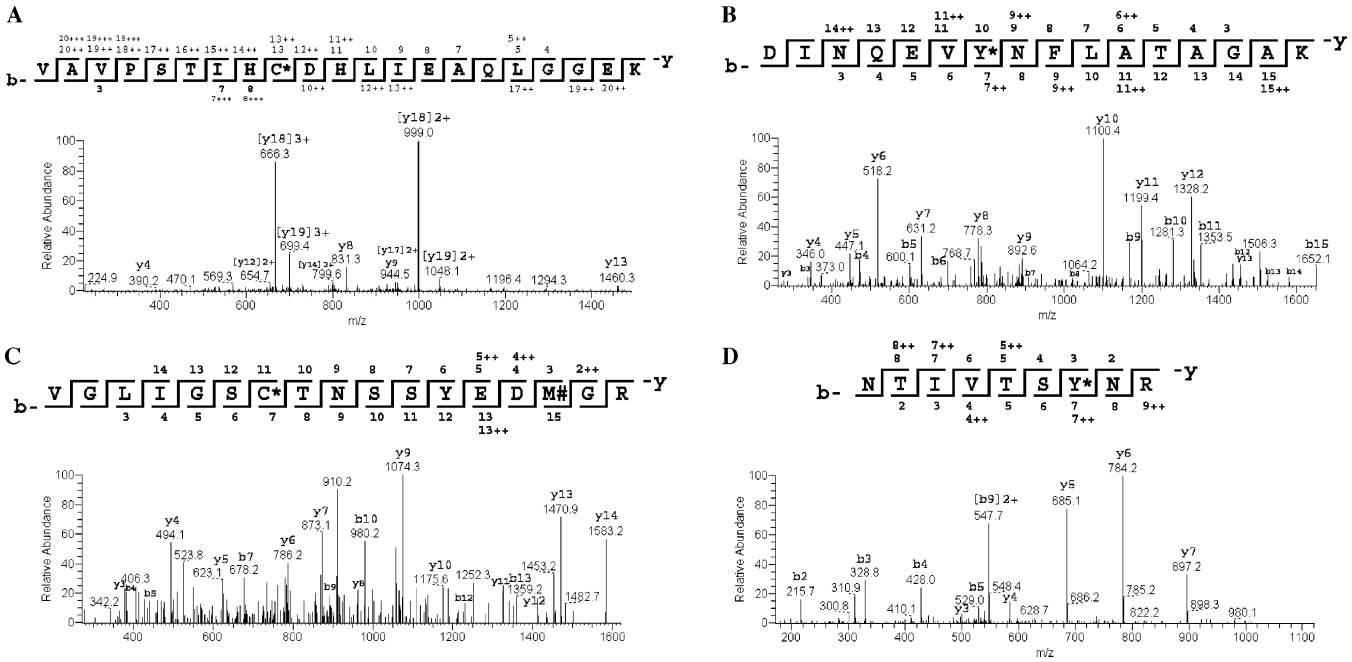

FIGURE 5: MS/MS spectra for aconitase tryptic peptides carrying an oxidative/nitrative modification. MS/MS spectra for peptides modified at (A) Cys^{126}, (B) Tyr^{151}, (C) Cys^{385}, and (D) Tyr^{472}. Charge state and identification scores are listed in Table 1. Above each spectra is the peptide sequence with observed b and y ions indicated by their fragmentation number above (y ions) or below (b ions) the sequence. ++ or +++ indicate doubly or triply charged ions. Single-charged ions are not designated with a +. The ion annotation is based upon results presented in Sequest's "display ions view" window that were corroborated by the dta file. Y* indicates a nitrotyrosine, C* indicates cysteine sulfonic acid or cysteic acid, and M# indicates oxidized methionine.

acid following $ONOO^-$ treatment in four separate sample analyses by LC/MS/MS. Each identification was based on the same doubly charged 17 amino acid tryptic peptide with consistent retention times among each LC/MS/MS run (data not shown). Sequest XC scores ranged from 4.0 to 4.6 with Δcn values of 0.59−0.66 (Table 1). A representative tandem MS/MS spectra (XC = 4.6) is shown in Figure 5C. Cysteic acid at position 385 observed in the doubly charged tryptic peptide corresponded to 17 amino acids, 379−395, of porcine aconitase. The precursor ion mass of 927.7 Da correlated with the cysteic acid modification and also a single oxidation at methionine 393, a commonly observed modification in tandem MS/MS analyses. The MS/MS collision-induced fragmentation pattern (Figure 5B) allowed near complete assignment of all observable single-charged b and y fragment ions and also included instances of doubly charged b and y ions.

Tyrosine 472. Nitration of tyrosine 472 was observed in three doubly charged nine amino acid tryptic peptides in two separate sample analyses by LC/MS/MS. Sequest XC values for the double-charged peptide ranged from 2.0 to 2.5 with Δcn values from 0.24 to 0.62 (Table 1). Retention times for the peptide were consistent among different LC/MS/MS runs. A representative MS/MS spectra is shown in Figure 5D (XC = 2.5). Precursor mass corresponding to the nitrotyrosine-modified double-charged tryptic fragment comprising aconitase residues 466−474 was 557.2 Da. The collision-induced ion fragmentation pattern included all observable single-charged b and y ions; two double-charged b and three double-charged y ions were also observed.

Cysteine 126. Modification of cysteine to cysteic acid at position 126 was observed 3 times, each in a separate LC/MS/MS analysis, in a triple-charged 21 amino acid length tryptic peptide that corresponded to aconitase residues 118−138. The Sequest XC and Δcn values ranged from 2.1 to 2.7 and 0.34 to 0.50, respectively. Retention times were consistent among different LC/MS/MS runs. The XC values are relatively low, with an XC value of 3 generally being considered the cutoff for assigning an identification of a triple-charged peptide. A representative MS/MS spectra is presented in Figure 5A (XC = 2.7). The precursor ion for the triple-charged peptide was 756.2 Da. The collision-induced fragmentation pattern shows a highly biased fragmentation where two major peaks dominate the spectra that correspond to double- and triple-charged y18 with the next two highest peaks corresponding to the double- and triple-charged y19. This biased fragmentation pattern where the double- and triple-charged y18 ions were by far the largest peaks with the y19 double and triple ions being the next highest set was consistently observed in several LC/MS/MS runs. Despite the abundance of the y18 and y19 ions, almost all of the observable y ions were assigned in either single- or double-charged state (sometimes both), and 9 of 21 total possible b ions were observed in either the double- or triple-charged state. The cysteine modification was observed in every possible double-charged y ion that would carry the modified cysteine (i.e., y13−y20).

Modulation of Aconitase Activity by GSSG. Cysteine and tyrosine residues in aconitase were affected by $ONOO^-$, and these modifications were associated with a decrease of aconitase activity. It may be hypothesized that cysteine thiol modifications other than oxidation to sulfonic acid (Figure 5) may similarly decrease aconitase activity. An important physiological thiol modification is glutathionylation of protein thiols by GSSG through disulfide−thiol exchange (*38*, *39*) (reaction 6).

$$\text{protein}-\text{SH} + \text{GSSG} \rightarrow \text{protein}-\text{SSG} + \text{GSH} \quad (6)$$

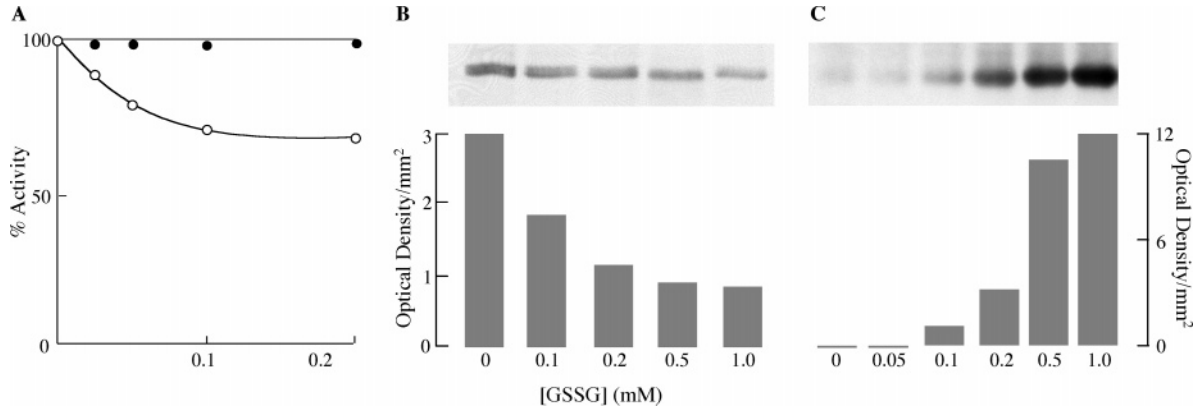

FIGURE 6: Effect of GSSG on aconitase activity and aconitase protein thiols. Glutathionylation of aconitase. (A) Effect of GSSG on aconitase activity. Various concentrations of GSSG were mixed with aconitase (2 mU/mL) in 50 mM Tris-HCl at pH 7.4 in the presence of 2.5 mM citrate for 10 min. (○) Aconitase plus GSSG. (●) Aconitase plus GSSG plus DTT. In the DTT-treated samples, aconitase was incubated with GSSG and citrate followed by a 10-min treatment with DTT (10 mM). (B) Western blots showing the loss of aconitase protein thiols following treatment with GSSG and the corresponding semiquantitative analysis (densitometry). (C) Western blots showing glutathionylation of aconitase, which was determined using an anti-glutathione monoclonal antibody as described in the Experimental Procedures, and the corresponding semiquantitative analysis (densitometry). Porcine aconitase (4 mU/mL) was rapidly mixed with varying amounts of GSSG in 50 mM Tris-HCl at pH 7.4 for 10 min.

Incubation of aconitase with GSSG in the presence of citrate led to a loss in enzyme activity (Figure 6A). Maximal inhibition (35%) was observed with ~200 μM GSSG. The loss of aconitase activity caused by GSSG corresponded with a decrease in protein-free thiols [as measured by Western blot analysis after maleimide PEO_2−biotin labeling (Figure 6B)], as expected upon protein thiol glutathionylation. The glutathionylation of aconitase was confirmed by Western blot analysis using a monoclonal antiglutathione antibody (Figure 6C), thus showing that GSSG glutathionylate aconitase in a dose-dependent manner. DTT, which reduces disulfide bonds to the corresponding thiols, fully reversed the loss of aconitase activity brought about by GSSG (Figure 6A).

These results demonstrate that aconitase activity can be modulated by glutathionylation and suggest that modification of cysteine residues outside the active site of aconitase can result in an impairment of enzyme activity.

DISCUSSION

Aconitase activity is frequently viewed as a marker of oxidative stress in biological systems because the enzyme $[4Fe-4S]^{2+}$ cluster is readily inactivated by $O_2^{\cdot-}$, H_2O_2, and $ONOO^-$. This study puts forward two mechanisms by which the Fe−S cluster in the active site could be modified by low levels of $ONOO^-$: (a) conversion of the active Fe−S cluster from the $[4Fe-4S]^{2+}$ form to the inactive $[3Fe-4S]^{1+}$ form with the loss of labile iron (as confirmed by low-temperature EPR analyses), and (b) disrupting the binding of the Fe−S cluster to cysteine residues (cysteine 385) of the protein through oxidation of cysteine to cysteic acid (as shown by LC/MS/MS analyses). However, whether the disruption in Fe−S binding to cysteine causes Fe−S degradation or the breakdown of the Fe−S cluster into the inactivate $[3Fe-4S]^{1+}$ form remains to be elucidated.

Binding of citrate to the aconitase active site selectively protected against modifications of the Fe−S cluster by $ONOO^-$, but this protection was not extended to amino acid residues (distal from or in close proximity to the active site). The mechanism by which citrate protects the Fe−S cluster from $ONOO^-$ probably involves inhibition of the entry of $ONOO^-$ to the Fe−S cluster upon citrate binding. In this regard, recent X-ray crystallography studies have shown that binding of citrate induces a conformational change of the aconitase active site (*1*). Hence, citrate may shield the Fe−S cluster against $ONOO^-$ attack by (a) sterically hindering access of reactive molecules to the Fe−S cluster or (b) causing a conformational shift of the active site that makes the Fe−S cluster less accessible to reactive molecules. It is likely that a combination of both mechanisms contributes to the effectiveness of citrate protection of the Fe−S cluster from oxidant attack. Whichever the mechanism underlying the protection by citrate, it may be surmised that citrate levels in the mitochondrial matrix will determine the site of $ONOO^-$ attack on aconitase by shifting $ONOO^-$ reactions from Fe−S clusters to cysteine, tyrosine, and other amino acid residues of aconitase. Physiological levels of citrate in the matrix are determined by the metabolic state of mitochondria, but in bacteria, citrate levels have been estimated in the millimolar range (*40*). If similar levels were to apply to mammalian mitochondria, the Fe−S cluster of aconitase may not be as vulnerable to oxidants as previously reported.

In the presence of citrate, the inhibitory effect of $ONOO^-$ suggested the occurrence of sensitive sites other than the Fe−S cluster-containing active site in the regulation of aconitase activity. LC/MS/MS analysis revealed that cysteine 385 (one of three cysteine residues that bind the Fe−S cluster in the active site of aconitase) was oxidized to cysteic acid and that three other amino acids (tyrosines 151 and 472 and cysteine 126) outside the active site were modified upon $ONOO^-$ treatment. The other two cysteines involved in cluster ligation are cysteines 448 and 451 (*41*). The crystal structure of porcine aconitase (*32*, *41*) indicates that all three modified amino acids (tyrosines 151 and 472 and cysteine 126) were adjacent to amino acids comprising the active site (parts A and B of Figure 7). Tyrosine 472, for example, lies as close as 3.86 Å to cysteine 451, which binds the Fe−S cluster (Figure 7B). Nitration of tyrosine 472 can greatly crowd the active site, thus diminishing the catalytic activity of aconitase. Thus, modifications to tyrosines 151 and 472 and cysteine 126, because of their close proximity to the

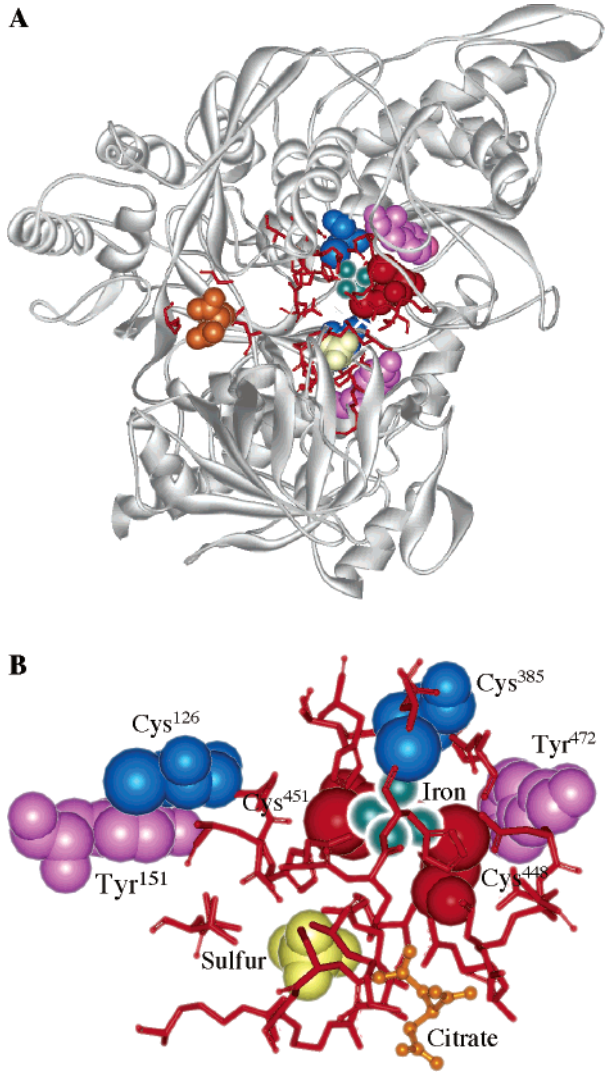

FIGURE 7: Structure of aconitase and amino acid modifications elicited by $ONOO^-$. (A) Full aconitase structure is illustrated in a ribbon format. Amino acid residues that compose the active site are shown in a stick format in red. Key molecules are illustrated in space-filling format: components of the Fe−S cluster (Fe shown in metallic green and sulfur shown in yellow), cysteine residues ligated to the Fe−S cluster (red), and citrate (orange). Cysteine residues oxidized to sulfonic acid (blue) (including modified cysteine 385 that binds the Fe−S cluster), and tyrosine residues converted to 3-nitrotyrosine (purple) by $ONOO^-$ treatment are also shown in space-filling format. (B) Close-up view of the active site with the same illustrative scheme as in A except that citrate is displayed in a stick configuration. The position of the view differs from that of A for the sake of clarity.

active site, may cause conformational changes that destabilize the active site. The oxidative reactions by $ONOO^-$ can take place by both one- and two-electron mechanisms (sequences in reactions 7 and 8, respectively) (*42*, *43*). The oxidation of cysteine residues (R−SH) in aconitase to sulfonic acid ($R-SO_3H$) involves oxidation steps beyond the initial formation of sulfenic acid (R−SOH) (reactions 1−3): these steps are likely to encompass another stable product, such as sulfinic ($R-SO_2H$) (reaction 7). Alternatively, the thiyl radical ($R-S^{\bullet}$), formed in reaction 1, can undergo further $ONOO^-$-mediated one-electron oxidations and reactions with molecular oxygen leading to cysteine sulfenic acid formation (sequence in reaction 8) (*44*) followed by similar reactions to sulfinic and sulfonic products.

$$R-SH \rightarrow R-SOH \rightarrow R-SO_2H \rightarrow R-SO_3H \quad (7)$$

$$R-SH \rightarrow R-S^{\bullet} \rightarrow R-SOH \rightarrow R-S^{\bullet}O \rightarrow R-SO_2H \rightarrow R-S^{\bullet}O_2 \rightarrow R-SO_3H \quad (8)$$

These conformational changes may account for the $ONOO^-$-mediated decrease in aconitase activity observed in the presence of citrate. Nonetheless, it remains to be determined whether there is one critical modification involved in the modulation of aconitase activity or whether all modifications contribute to the loss of aconitase activity. However, on the basis of the sensitivity of aconitase to glutathionylation, cysteine modifications appear to be more critical than tyrosine modifications in modulating aconitase activity. The loss of aconitase after GSSG treatment suggests glutathionylation of one or more cysteine residues may cause conformational changes that affect enzyme activity, and thiols may be required to stabilize a protein structure associated with the function.

This study provides the first evidence that aconitase is susceptible to glutathionylation and that this process may modulate aconitase activity. These findings suggest that glutathionylation of aconitase may be an important means of modulating aconitase activity under oxidative and nitrosative stress. The mitochondrial matrix contains high levels of GSH, which is believed to scavenge $ONOO^-$ and protect sensitive enzymes such as aconitase. However, GSSG is the major end product (*45*) originating from the reaction between GSH and $ONOO^-$ (reaction 9−11), thus providing a reactant for protein-mixed disulfide formation (reaction 6).

$$GSH + [HO^{\bullet}\cdots NO_2^{\bullet}] \rightarrow GS^{\bullet} + {}^{\bullet}NO_2 + OH^- \quad (9)$$

$$GS^- + GS^{\bullet} \rightarrow GSSG^{\bullet -} \quad (10)$$

$$GSSG^{\bullet -} + O_2 \rightarrow GSSG + O_2^{\bullet -} \quad (11)$$

$ONOO^-$ formation in the mitochondrial matrix may therefore modulate aconitase activity in two ways: (a) directly, upon modifications of the Fe−S cluster and/or critical amino acids residues, and/or (b) indirectly, through oxidation of mitochondrial GSH to GSSG, which in turn can lead to gluathionylation of aconitase. Because of the high levels of GSH in mitochondria, glutathionylation of aconitase would appear as a major physiological consequence of $ONOO^-$ formation in the mitochondrial matrix. Mitochondrial GSH may have other functions, because it was reported that the recovery of aconitase activity ($[3Fe-4S]^{1+} \rightarrow [4Fe-4S]^{2+}$) was accomplished *in vivo* by a process involving GSH (*46*) or the iron chaperone protein frataxin (*47*). Of note, citrate, in addition to sterically protecting the active site, plays an important role in repair of the Fe−S cluster. The inactive $[3Fe-4S]^{1+}$ cluster, formed upon oxidant attack, is repaired by frataxin; an iron-binding protein and recent studies (*5*, *47*) have shown that citrate is required to stabilize the frataxin−aconitase interaction so that iron is reinserted to form the active $[4Fe-4S]^{2+}$ cluster. In the absence of citrate, aconitase is not effectively repaired in mitochondria following oxidative challenge and remains inactive. This suggests that citrate levels may be an important factor in modulating aconitase activity during oxidative stress.

It may be surmised that [GSH]/[GSSG] ratios in the mitochondrial matrix are important factors that determine aconitase functionality. GSSG levels are tightly regulated in mitochondria, and GSSG is rapidly reduced to GSH by glutathione reductase. This indicates that aconitase activity is finely regulated by the mitochondrial metabolic and redox states, which determine citrate and NADPH levels, with the latter closely tied to GSSG level regulation. Reactive oxygen and nitrogen species levels, citrate concentration, and the [GSH]/[GSSG] ratio may be intrinsically involved in the regulation of aconitase activity in mitochondria, and the sites and mechanisms of inactivation will be determined by the interaction of these factors. Thus, the metabolic and thiol redox status of the mitochondrial matrix may play an important role in the physiological regulation of aconitase activity.

ACKNOWLEDGMENT

We thank Dr. Daniel Rettori for his help with experiments involving EPR.

REFERENCES

1. Lauble, H., and Stout, C. D. (1995) Steric and conformational features of the aconitase mechanism, *Proteins 22*, 1−11.
2. Beinert, H., and Kennedy, M. C. (1993) Aconitase, a two-faced protein: enzyme and iron regulatory factor, *FASEB J. 7*, 1442−1449.
3. Gardner, P., and Fridowich, I. (1991) Superoxide sensitivity of the *Escherichia coli* aconitase, *J. Biol. Chem. 266*, 19328−19333.
4. Castro, L., Rodriguez, M., and Radi, R. (1994) Aconitase is readily inactivated by peroxynitrite, but not by its precursor, nitric oxide, *J. Biol. Chem. 269*, 29409−29415.
5. Bulteau, A. L., Ikeda-Saito, M., and Szweda, L. I. (2003) Redox-dependent modulation of aconitase activity in intact mitochondria, *Biochemistry 42*, 14846−14855.
6. Gardner, P. R., and Fridovich, I. (1992) Inactivation−reactivation of aconitase in *Escherichia coli*. A sensitive measure of superoxide radical, *J. Bio. Chem. 267*, 8757−8763.
7. Nulton-Persson, A. C., and Szweda, L. I. (2001) Modulation of mitochondrial function by hydrogen peroxide, *J. Biol. Chem. 276*, 23357−23361.
8. Kennedy, M. C., Spoto, G., Emptage, M. H., and Beinert, H. (1988) The active site sulphydryl of aconitase is not required for catalytic activity, *J. Biol. Chem. 263*, 8190−8193.
9. Radi, R., Beckman, J. S., Bush, K. M., and Freeman, B. A. (1991) Peroxynitrite oxidation of sulphydryls, *J. Biol. Chem. 266*, 4244−4250.
10. Carballal, S., Radi, R., Kirk, M. C., Barnes, S., Freeman, B. A., and Alvarez, B. (2003) Sulfenic acid formation in human serum albumin by hydrogen peroxide and peroxynitrite, *Biochemistry 42*, 9906−9914.
11. Radi, R., Cassina, A., Hodara, R., Quijano, C., and Castro, L. (2002) Peroxynitrite reactions and formation in mitochondria, *Free Radical Biol. Med. 33*, 1451−1464.
12. Hausladen, A., and Fridovich, I. (1996) Measuring nitric oxide and superoxide: Rate constant for aconitase reactivity, *Methods Enzymol. 269*, 37−41.
13. Cadenas, E., and Boveris, A. (1980) Enhancement of hydrogen peroxide formation by protophores and ionophores in antimycin-supplemented mitochondria, *Biochem. J. **188***, 31−37.
14. Han, D., Antunes, F., Daneri, F., and Cadenas, E. (2002) Mitochondrial superoxide anion production and release into intermembrane space, *Methods Enzymol. 349*, 271−280.
15. Elfering, S. L., Sarkela, T. M., and Giulivi, C. (2002) Biochemistry of mitochondrial nitric-oxide synthase, *J. Biol. Chem. 277*, 38079−38086.
16. Riobó, N. A., Melani, M., Sanjuan, N., Fiszman, M. L., Gravielle, M. C., Carreras, M. C., Cadenas, E., and Poderoso, J. J. (2002) The modulation of mitochondrial nitric-oxide synthase activity in rat brain development, *J. Biol. Chem. 277*, 42447−42455.
17. Ghafourifar, P., and Cadenas, E. (2005) Mitochondrial nitric oxide synthase, *Trends Pharmacol. Sci. 26*, 190−195.
18. Torres, J., Darley-Usmar, V., and Wilson, M. T. (1995) Inhibition of cytochrome *c* oxidase in turnover by nitric oxide: Mechanism and implications for control of respiration, *Biochem. J. 312*, 169−173.
19. Brown, G. C. (1997) Nitric oxide inhibition of cytochrome oxidase and mitochondrial respiration: Implications for inflammatory, neurodegenerative, and ischaemic pathologies, *Mol. Cell Biochem. 174*, 189−192.
20. Antunes, F., Boveris, A., and Cadenas, E. (2004) On the mechanism and biology of cytochrome oxidase inhibition by nitric oxide, *Proc. Natl. Acad. Sci. U.S.A. 101*, 16774−16779.
21. Poderoso, J. J., Carreras, M. C., Lisdero, C., Riobo, N., Schopfer, F., and Boveris, A. (1996) Nitric oxide inhibits electron transfer and increases superoxide radical production in rat heart mitochondria and submitochondrial particles, *Arch. Biochem. Biophys. 328*, 85−92.
22. Cadenas, E., Poderoso, J. J., Antunes, F., and Boveris, A. (2001) Analysis of the pathways of nitric oxide utilization in mitochondria, *Free Radical Res. 33*, 747−756.
23. Riobó, N. A., Clementi, E., Melani, M., Boveris, A., Cadenas, E., Moncada, S., and Poderoso, J. J. (2001) Nitric oxide inhibits mitochondrial NADH-ubiquinone reductase activity through the formation of peroxynitrite, *Biochem. J. 359*, 139−145.
24. Schopfer, F., Riobo, N. A., Carreras, M. C., Alvarez, B., Radi, R., Boveris, A., Cadenas, E., and Poderoso, J. J. (2000) Oxidation of ubiquinol by peroxynitrite: Implications for protection of mitochondria against nitrosative damage, *Biochem. J. 349*, 35−42.
25. Brookes, P. S., Levonen, A.-L., Shiva, S., Sarti, P., and Darley-Usmar, V. M. (2002) Mitochondria: Regulators of signal transduction by reactive oxygen and nitrogen species, *Free Radical Biol. Med. 33*, 755−764.
26. Packer, M. A., and Murphy, M. P. (1994) Peroxynitrite causes calcium efflux from mitochondria which is prevented by cyclosporin A, *FEBS Lett. 345*, 237−240.
27. Beckman, J., and Koppenol, W. H. (1996) Nitric oxide, superoxide, and peroxynitrite: The good, the bad, and the ugly, *Am. J. Physiol. 261*, H590−H597.
28. Han, D., Antunes, F., Canali, R., Rettori, D., and Cadenas, E. (2003) Voltage-dependent anion channels control the release of the superoxide anion from mitochondria to cytosol, *J. Biol. Chem. 278*, 5557−5563.
29. Gardner, P., Costantino, G., Szabo, C., and Salzam, A. L. (1997) Nitric oxide sensitivity of the aconitase, *J. Biol. Chem. 272*, 25071−25076.
30. Drapier, J. C., and Hibbs, J. B. (1996) Aconitases: A class of metalloproteins highly sensitive to nitric oxide synthesis, *Methods Enzymol. 269*, 26−36.
31. Wang, J., Boja, E. S., Tan, W., Tekle, E., Fales, H. M., English, S., Mieyal, J. J., and Chock, P. B. (2001) Reversible glutathionylation regulates actin polymerization in A431 cells, *J. Biol. Chem. 276*, 47763−47766.
32. Robbins, A. H., and Stout, C. D. (1989) Structure of activated aconitase: Formation of the [4Fe−4S] cluster in the crystal, *Proc. Natl. Acad. Sci. U.S.A. 86*, 3639−3643.
33. Duling, D. R. (1994) Simulation of multiple isotropic spin-trap EPR spectra, *J. Magn. Reson. Ser. B 104*, 105−110.
34. Kennedy, M. C., Antholine, W. E., and Beinert, H. (1997) An EPR investigation of the products of the reaction of cytosolic and mitochondrial aconitase with nitric oxide, *J. Biol. Chem. 272*, 20340−20347.
35. Haddad, I. Y., Crow, J. P., Hu, P., Ye, Y., Beckman, J., and Matalon, S. (1994) Concurrent generation of nitric oxide and superoxide damages furfactant protein A, *Am. J. Physiol. 267*, L242−L249.
36. Maples, K. R., Jordan, S. J., and Mason, R. P. (1988) *In vivo* rat hemoglobin thiyl free radical formation following phenylhydrazine administration, *Mol. Pharmacol. 33*, 344−350.
37. Augusto, O., Menezes, L. d., Linares, E., Romero, N., Radi, R., and Denicola, A. (2002) EPR detection of glutathiyl and hemoglobin-cysteinyl radicals during the interaction of peroxynitrite with human erythrocytes, *Biochemistry 41*, 14323−14328.
38. Thomas, J. A., Poland, B., and Honzatko, R. (1995) Protein sulfhydryls and their role in the antioxidant function of protein S-thiolation, *Arch. Biochem. Biophys. 319*, 1−9.

39. Gilbert, H. F. (1982) Biological disulfides: The third messenger? Modulation of phosphofructokinase activity by thiol/disulfide exchange, *J. Biol. Chem. 257*, 12086−12091.
40. Lowry, O. H., Carter, J., Ward, J. B., and Glaser, L. (1971) The effect of carbon and nitrogen sources on the level of metabolic intermediates in *Escherichia coli*, *J. Biol. Chem. 246*, 6511−6521.
41. Lauble, H., Kennedy, M. C., Beinert, H., and Stout, C. D. (1992) Crystal structures of aconitase with isocitrate and nitroisocitrate bound, *Biochemistry 31*, 2735−2748.
42. Goldstein, S., and Czapski, G. (1995) Direct and indirect oxidation by peroxynitrite, *Inorg. Chem. 34*, 4401−4048.
43. Koppenol, W., Moreno, J., Pryor, W., Ischiropoulos, H., and Beckman, J. S. (1992) Peroxynitrite, a cloaked oxidant formed by nitric oxide and superoxide, *Chem. Res. Toxicol. 5*, 834−842.
44. Harman, L. S., Mottley, C., and Mason, R. P. (1984) Free radical metabolites of L-cysteine oxidation, *J. Biol. Chem. 259*, 5606−5611.
45. Radi, R., Beckman, J. S., Bush, K. M., and Freeman, B. A. (1991) Peroxynitrite oxidation of sulfhydryls. The cytotoxic potential of superoxide and nitric oxide, *J. Biol. Chem. 266*, 4244−4250.
46. Gardner, P. R., and Fridovich, I. (1993) Effect of glutathione on aconitase in *Escherichia coli*, *Arch. Biochem. Biophys. 301*, 98−102.
47. Bulteau, A. L., O'Neill, H. A., Kennedy, M. C., Ikeda-Saito, M., Isaya, G., and Szweda, L. I. (2004) Frataxin acts as an iron chaperone protein to modulate mitochondrial aconitase activity, *Science 305*, 242−245.

BI0509393